Influence of Cellulose on Ion Diffusivity in 1-Ethyl-3-Methyl-Imidazolium Acetate Cellulose Solutions

ARTICLE *in* BIOMACROMOLECULES · OCTOBER 2010

Impact Factor: 5.75 · DOI: 10.1021/bm1006807 · Source: PubMed

7 AUTHORS, INCLUDING:

Christopher S Lovell

5 PUBLICATIONS **76** CITATIONS

SEE PROFILE

Robin A. Damion

16 PUBLICATIONS **156** CITATIONS

SEE PROFILE

Steven F Tanner

Leeds Teaching Hospitals NHS Trust

71 PUBLICATIONS **2,386** CITATIONS

SEE PROFILE

Tatiana Budtova

MINES ParisTech

120 PUBLICATIONS **1,411** CITATIONS

SEE PROFILE

Influence of Cellulose on Ion Diffusivity in 1-Ethyl-3-Methyl-Imidazolium Acetate Cellulose Solutions

Christopher S. Lovell,[†] Adam Walker,[†] Robin A. Damion,[†] Asanah Radhi,[†] Steven F. Tanner,[‡] Tatiana Budtova,[§] and Michael E. Ries*[,†]

IRC in Polymer Science and Technology, School of Physics and Astronomy, University of Leeds, Leeds, LS2 9JT United Kingdom, Academic Division of Medical Physics, University of Leeds, Leeds, LS2 9JT United Kingdom, and Centre de Mise en Forme des Materiaux, UMR CNRS 7635, rue Claude Daunesse, BP 207, 06904 Sophia Antipolis, France

Received June 18, 2010; Revised Manuscript Received September 15, 2010

Solutions of microcrystalline cellulose in 1-ethyl-3-methyl-imidazolium acetate have been investigated using pulsed-field gradient ^{1}H NMR. In all cases the geometrically larger cation was found to diffuse faster than the smaller anion. Arrhenius temperature analysis has been applied to the ion diffusivities giving activation energies. The diffusion and published viscosity data for these solutions were shown to follow the Stokes−Einstein relationship, giving hydrodynamic radii of 1.6 Å (cation) and 1.8 Å (anion). Theories for obstruction, free-volume and hydrodynamic effects on solvent diffusion have been applied. The Mackie−Meares and Maxwell−Fricke obstruction models provided a correct trend only when assuming a certain fraction of ions are bound to the polymer. From this fraction it was shown that the maximum dissolvable cellulose concentration is ∼27% w/w, which is consistent with the highest known prepared concentration of cellulose in this ionic liquid. The Phillies' hydrodynamic model is found to give the best description for the cellulose concentration dependence of the ion diffusivities.

1. Introduction

Sustainable resources and green cost-effective technologies are of clear importance for the future of polymer science and industry.[1] Cellulose is the most abundant naturally occurring polymer and is a practically inexhaustible resource for the production of environmentally friendly, biodegradable, and biocompatible products.[2] Despite these advantages the full potential of cellulose has not yet been realized commercially. Foremost cellulose is an intractable solid due to strong inter- and intramolecular hydrogen bonds and so requires the use of chemicals with undesirable properties to provide viable solutions for industrial processes. For example the highly volatile and toxic carbon disulfide is used in the viscose process.[3] Over the last few decades *N*-methylmorpholine *N*-oxide monohydrate (NMMO),[4] LiCl/*N*,*N*-dimethylacetamide,[5] alkylammonium fluoride/dimethylsulfoxide (DMSO),[6] molten salt hydrates,[7,8] aqueous NaOH[9] and NaOH/urea[10] solutions, and both ammonia[11] and ethylenediamine[12] thiocyanate salt solutions have been investigated as alternatives to the traditional cellulose solvents. However environmental and economic issues have limited their industrial development. Only NMMO is used commercially in the production of cellulose fibres (Lyocell process). This process though is somewhat disadvantaged by side-reactions[13] and high dissolution temperatures. There is therefore a strong incentive to develop new "green" solvents for cellulose regeneration and derivatization.

Ionic liquids (ILs) are an emerging class of versatile materials which have rapidly gained interest from both industry and academia due to their considerable potential for developments in green chemistry and as novel electrolytes for electrochemical devices.[14–17] Research has been driven by their unique properties of negligible vapor pressure, nonflammability, high ionic conductivity, high thermal and electrochemical stability, and the ability to tailor their physical properties through changes in cation and anion chemical structures.[14,18] Specifically the absence of a measurable vapor pressure and good dissolution properties for a variety of inorganic and organic materials mean that ILs are now being exploited extensively in revising traditional chemical processes.[16,19]

Imidazolium based ILs such as 1-ethyl-3-methyl-imidazolium acetate (EMIMAc) have been found to be cellulose nonderivatizing solvents[20] that provide sufficient solvation capabilities to yield cellulose concentrations practical for industrial purposes. Research in the characterization of cellulose/IL solutions and the practical implementation of these systems has been summarized in recent reviews.[3,17,20–25]

Nuclear magnetic resonance (NMR) spectroscopy has been applied extensively in the characterization of ILs, for example, to examine structural organization and phase behavior in aqueous solutions,[26] ionicity,[27] ion diffusivities,[28] and ion−solute interactions.[29] A few NMR studies have also been published on model cellulose/IL solutions, in particular to address the mechanism by which ions mediate cellulose dissolution and solvation.[30,31] The understanding of the microscopic properties (polymer−solvent interactions, transport) of cellulose-IL solutions will lead to a better control of the dissolution process and of the final materials properties. It is therefore important to quantify the relationship between the self-diffusion coefficients, and hence ion mobility, and the viscosity and concentration of cellulose in ILs. Zhang et al.[31] recently reported ^{1}H and ^{13}C NMR studies of cellobiose solvation in EMIMAc. Their analysis of the concentration dependences of both ^{1}H and ^{13}C chemical shifts for cellobiose and EMIMAc lead to the firm conclusion that there exists hydrogen bonding interactions between the cellulose hydroxyl groups and both the $[EMIM]^+$ and $[Ac]^-$

* To whom correspondence should be addressed. E-mail: m.e.ries@leeds.ac.uk.
[†] School of Physics and Astronomy, University of Leeds.
[‡] Academic Division of Medical Physics, University of Leeds.
[§] UMR CNRS 7635.

10.1021/bm1006807
Published on Web 10/05/2010

ions. It was concluded that the hydrogen atoms of the cellulose hydroxyl groups are stronger hydrogen bond donors than the hydrogen atoms associated with the imidazolium ring. Therefore the hydroxyl groups favorably displace the $[EMIM]^+$ ions forming stronger hydrogen bonds with the $[Ac]^-$ ions. The $[EMIM]^+$ ions then establish weaker hydrogen bonds with oxygen atoms in the cellulose hydroxyl groups, due to their lower hydrogen bonding acceptor ability (as compared to the $[Ac]^-$). In this manner a process in which ions coordinate with the cellulose hydroxyl groups can account for the solvation properties of EMIMAc.

Pulsed field gradient (PFG) NMR techniques are a set of noninvasive methods for measuring molecular self-diffusion coefficients,[32] which among other techniques such as fluorescence correlation spectroscopy have been used extensively in the analysis of polymer−solvent systems. Using diffusion-ordered two-dimensional NMR spectroscopy (DOSY) it is possible to identify the molecular components of mixtures and simultaneously measure their self-diffusion coefficients.[33]

In this paper we present results of ^{1}H NMR spectroscopic and DOSY measurements obtained from pure EMIMAc and a series of cellulose/EMIMAc solutions of various concentrations and at different temperatures. To the best of our knowledge this is the first paper that uses NMR to look at the diffusion of an ionic liquid in a cellulose/IL solution. We analyze the change in the chemical shifts of each EMIMAc spectral band and determine the diffusion coefficients of each ion, $[EMIM]^+$ and $[Ac]^-$. The influence of solution temperature and cellulose concentration on ion mobility is discussed. Different theoretical approaches that exist for the analysis of solvent diffusion in a polymer solution are applied to our experimental data in order to model the ion transport properties in the presence of cellulose. EMIMAc was chosen as a real room-temperature ionic liquid which is liquid at ambient conditions. The temperature interval was thus chosen as 10−70 °C to avoid cellulose degradation at higher temperatures.[34]

2. Experimental Section

2.1. Materials and Sample Preparation. EMIMAc (purity ≥97%) was purchased from Sigma-Aldrich and used as received without further purification. Avicel PH-101 microcrystalline cellulose ("cellulose" in the following) was purchased from FMC Corporation; the degree of polymerization is 180 as given by the manufacturer. Cellulose was dried under vacuum at 100 °C for a period of 24 h prior to use.

Dissolution was achieved under stirring in an MBraun Labmaster 130 Atmospheric Chamber under nitrogen at 80 °C for at least 48 h. The chamber is maintained at a dewpoint level between −70 and −40 °C. In this work pure EMIMAc and five cellulose/EMIMAc solutions with 1%, 3%, 5%, 10%, and 15% (*w*/*w*) were studied in the temperature range 10−70 °C. A small quantity of each cellulose/EMIMAc solution was placed in a standard 5 mm NMR tube within the chamber. Each tube was subsequently sealed within the chamber to prevent moisture contamination and when the samples were not in use they were stored in a desiccator. From the ^{1}H NMR spectra we estimate the water content of our samples to be less than 0.5% (*w*/*w*).

2.2. Pulsed-Field Gradient ^{1}H NMR Spectroscopy. Self-diffusion coefficients of both the $[EMIM]^+$ and $[Ac]^-$ ions (see Figure 1) were determined by a pulsed-field gradient ^{1}H NMR technique using a wide-bore Avance II NMR Spectrometer (Bruker Biospin) operating at a proton resonant frequency of 400 MHz. A specialized Diff60 diffusion probe (Bruker Biospin) capable of producing a maximum field gradient of 24 T m^{-1} was employed in the experiments. The calibration of the gradient field strength was performed by measuring the self-diffusion coefficient of water at 20.0 ± 0.1 °C which has the value (2.03 ± 0.01) × 10^{-9} m^2 s^{-1}. A subsequent calibration of the sample

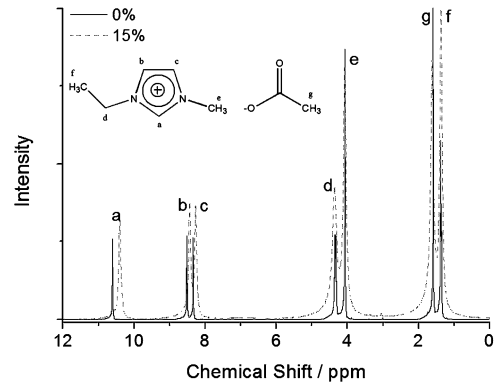

Figure 1. ^{1}H NMR spectra of pure EMIMAc (solid line) and 15% cellulose/EMIMAc solution (dashed line) obtained at 20 °C. The inset shows the chemical structure of $[EMIM]^+$ and $[Ac]^-$ ions of 1-ethyl-3-methyl-imidazolium acetate.

environment temperature was performed by measuring the temperature dependence of the diffusion coefficient of water with reference to results published by Holz et al.[35] The recommendations set out by Annat et al. for the NMR diffusion measurements of ionic liquids were followed.[36]

In this work we used a stimulated echo pulse sequence with bipolar gradients. The attenuation of the signal intensity in this PFG NMR experiment is given by[37]

$$\ln(S_i/S_{i0}) = -D_i\gamma^2 g^2 \delta^2(\Delta - \delta/3 - \tau/2) \quad (1)$$

where S_i is the measured signal intensity of species i, D_i is the self-diffusion coefficient of that species, S_{i0} defines the initial signal intensity, γ is the proton gyromagnetic ratio, δ is the pulse duration of a combined pair of bipolar pulses, τ is the period between bipolar gradients, Δ is the period separating the beginning of each pulse-pair (i.e., diffusion time), and g is the gradient strength. In each individual experiment the strength of the gradient pulse was incremented while δ and Δ remained constant. However it was necessary to increase the values for δ and Δ with increasing concentration of the cellulose solutions in order to capture the complete attenuation of the signal intensity. τ was kept constant at 2 ms.

3. Results and Discussions

3.1. ^{1}H NMR Spectra and Evidence for Hydrogen Bonding. A comparison between ^{1}H NMR spectra obtained at 20 °C for the pure IL and the 15% cellulose/EMIMAc solution is shown in Figure 1. Assignments of the spectral bands, which are labeled a−g, are made with reference to the chemical structure of EMIMAc shown in Figure 1. Due to the relatively small population of protons associated with the polymer in the concentration ranges investigated and the additional effect of ^{1}H−^{1}H dipolar broadening the cellulose spectral bands are therefore not observed in the NMR spectra. Interactions between the ions and cellulose are clearly evident through the concentration dependences of the spectral band chemical shifts for both $[EMIM]^+$ and $[Ac]^-$ species.

As seen in Figure 1 each spectral band is well-resolved and can be identified with a specific ^{1}H species within the EMIMAc structure. Despite the intrinsic ionic nature of EMIMAc multiple spectral bands for each ^{1}H species (i.e., a−g), which may indicate associated and dissociated ion states, are not observed. Thus any exchange between isolated ions, ion pairs and ion aggregates (assuming their presence) must occur on a time-scale shorter than that set by the experiment (i.e., 10^{-8}−10^{-9} s).

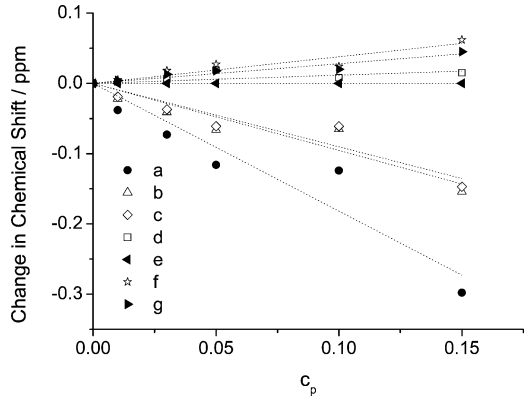

Figure 2. Concentration dependence of the change in ^{1}H NMR chemical shift for each EMIMAc spectral band. The dashed lines are presented as an aid-to-the-eye. The error bars are approximately equal to the size of the data points used.

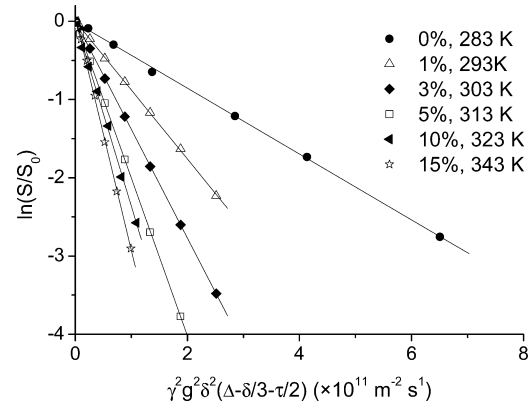

Figure 3. Gradient attenuation of the f spectral band intensity associated with the $[EMIM]^+$ ion. Various temperatures and concentrations are shown to illustrate that eq 1 holds for all our data. The error bars are approximately equal to the size of the data points used.

Ionicity is considered to be an important parameter in determining the physical properties of ILs.[27] It can be probed by infrared and Raman spectroscopy,[38] and by comparing the molar conductivity obtained by electrochemical impedance measurements with measurements of the ion self-diffusion coefficients through the application of the Nernst−Einstein equation.[27] In this respect it is important to recognize that the measured ^{1}H NMR spectrum is representative of the dynamic equilibrium which exists between associated and dissociated ions.

In Figure 2 we present the dependence of the change in chemical shift (relative to the pure IL) on cellulose concentration observed at 20 °C for each of the EMIMAc spectral bands. In our analysis spectral band e was defined to have a fixed chemical shift independent of the cellulose concentration as a point of reference. This choice follows several different ^{1}H NMR studies on imidazolium based ILs where the chemical shift of the methyl group (i.e., spectral band 'e') has been shown to be largely independent of extrinsic variables, such as IL concentration in water/1-alkyl-3-methylimidazolium bromide solutions[26] and cellobiose concentration upon solvation in EMIMAc.[31]

The concentration dependence of the chemical shifts observed for the series of the cellulose/EMIMAc solutions is in fact very similar to the behavior reported by Zhang et al.[31] for the solvation of cellobiose in EMIMAc. It follows that our results are therefore consistent with their proposed mechanism for cellulose dissolution and solvation through the coordination of $[EMIM]^+$ and $[Ac]^-$ ions with cellulose hydroxyl groups.

In the subsequent sections, the temperature and concentration dependences of the $[EMIM]^+$ and $[Ac]^-$ ion diffusivities are presented. From the above results the consideration of interactions between cation, anion and cellulose are of clear importance for their interpretation.

3.2. Determination of Self-Diffusion Coefficients of $[EMIM]^+$ and $[Ac]^-$ Species in EMIMAc and Cellulose/EMIMAc Solutions. In Figure 3 a selection of experimental data for the f spectral band intensity of $[EMIM]^+$ ion demonstrates, in accordance with eq 1, that a linear relationship was observed in the attenuation of the signal intensities. This was found to be true for all spectral bands at all temperatures and concentrations. This linear result is significant as this means that on the time-scale of the diffusion measurements (10 − 60 ms) the ions may be considered to experience a homogeneous solution environment. There is no evidence for phase separation and specifically we do not observe biexponential decays, which would indicate structurally distinct regions with different characteristic diffusivities. This result is consistent with the

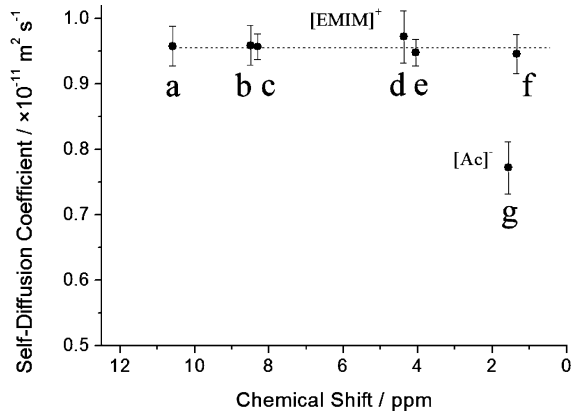

Figure 4. Self-diffusion coefficients evaluated from the gradient attenuation of each spectral band for pure EMIMAc at 20 °C. The average diffusion coefficient of $[EMIM]^+$ is shown by the dashed line.

rheology of cellulose/EMIMAc solutions.[39] It was shown that at low shear rates there is a broad Newtonian plateau and at high shear rates there is a single shear-thinning region, this being the same as for conventional isotropic homogeneous polymeric fluids.

The self-diffusion coefficients were calculated from the slope of each data set for each spectral band (a−g). The results obtained for the pure IL at 20 °C are presented in Figure 4. As expected the diffusion coefficients for the bands a−f, which are associated with the $[EMIM]^+$ ion, all have the same value since they are attached to the same diffusing molecule, whereas band g, which is associated with the $[Ac]^-$ ion, has a different diffusion coefficient. A clear contrast is therefore observed in the diffusive behavior of $[EMIM]^+$ and $[Ac]^-$ species. At 20 °C for the pure IL this can be characterized by the following self-diffusion coefficients $D_{EMIM} = (9.6 \pm 0.2) \times 10^{-12}$ m^2 s^{-1} (i.e., the horizontal dashed line in Figure 4) and $D_{Ac} = (7.7 \pm 0.4) \times 10^{-12}$ m^2 s^{-1}. The same procedure of diffusion coefficients determination for the other temperatures and cellulose concentrations was performed. In the subsequent sections we report the diffusion coefficient for the $[Ac]^-$ ion and the averaged value across a−f for the $[EMIM]^+$ ion.

As in previous NMR studies[28,40–42] on several imidazolium based ILs, the smaller anion is observed to diffuse at a rate slower than the larger cation. Recent molecular dynamics simulations modeling ILs have qualitatively reproduced the

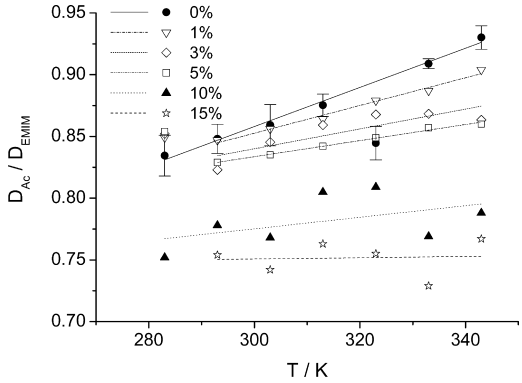

Figure 5. Temperature dependence of the ratio of $[Ac]^-$ to $[EMIM]^+$ diffusivities at various cellulose concentrations. Solid and dashed lines correspond to linear approximations. For clarity we have only displayed error bars for the pure EMIMAc data, the uncertainties in the other results are of a similar size.

quicker self-diffusion of the larger cation species for several systems.[43,44] There are three principal factors which determine ion diffusivities: ion size, ion shape, and the magnitude of ion interaction energies.[26] Urahata and Ribeiro[44] conclude from their computer simulations that the faster diffusion of the larger imidazolium ions may be explained by anisotropic diffusion. Specifically their analysis demonstrated that the mean-square displacement evaluated in the direction which lies in the imidazolium ring-plane and perpendicular to the long-axis of the alkyl chain (recall Figure 1) was larger than the displacements evaluated in orthogonal directions.

The contrast in ion diffusivities is examined further in Figure 5 by showing the temperature and concentration dependences of the ratio of cation to anion diffusion coefficients. In previous studies on imidazolium, pyridinium and pyrrolidinium based ILs it has been observed that at higher temperatures the diffusivities of both the cation and anion species generally tend toward the same value.[28,40–42] This trend is observed most noticeably for pure EMIMAc (see 0% data in Figure 5). In contrast for the cellulose solutions the ratios of the ion diffusivities display weaker temperature dependences. Indeed for the 15% solution the ratio remains at an approximately constant value, $D_{Ac}/D_{EMIM} \approx 0.75$, across the range of temperatures investigated. The disparity between the cation and anion self-diffusion coefficients increases with increasing cellulose concentration. The addition of cellulose must alter the ion interaction energies in such a way as to further increase the difference between the counterion diffusivities.

3.3. Influence of Temperature on Ions Diffusion. Further information may be ascertained from the temperature dependences of the ion diffusivities by considering the absolute values of the self-diffusion coefficients (Figure 6a,b). In earlier rheological studies[39] of EMIMAc and cellulose/EMIMAc solutions the dependences of the solution zero-shear viscosities on the inverse temperature (in the range 0−100 °C) were found to be concave, and the Vogel−Tamman−Fulcher (VTF) equation for glass-forming liquids was used to fit the viscosity-temperature data. The temperature range in our study is narrower and the data does not show sufficient curvature on a ln D versus $1/T$ plot; therefore, an Arrhenius analysis was applied

$$D_i(T) = D_{iA} \exp(-E_{iA}/RT) \qquad (2)$$

where E_{iA} is the activation energy of the i species and R is the gas constant. As seen from the fits presented in Figure 6, panels a and b, the Arrhenius analysis provides an excellent approximation with R^2 typically greater than 0.99 for the temperature dependences in the studied range. It is expected that for a wider temperature interval the VTF behavior would become more evident. Values obtained for the parameters D_{iA} and E_{iA} are listed in Table 1.

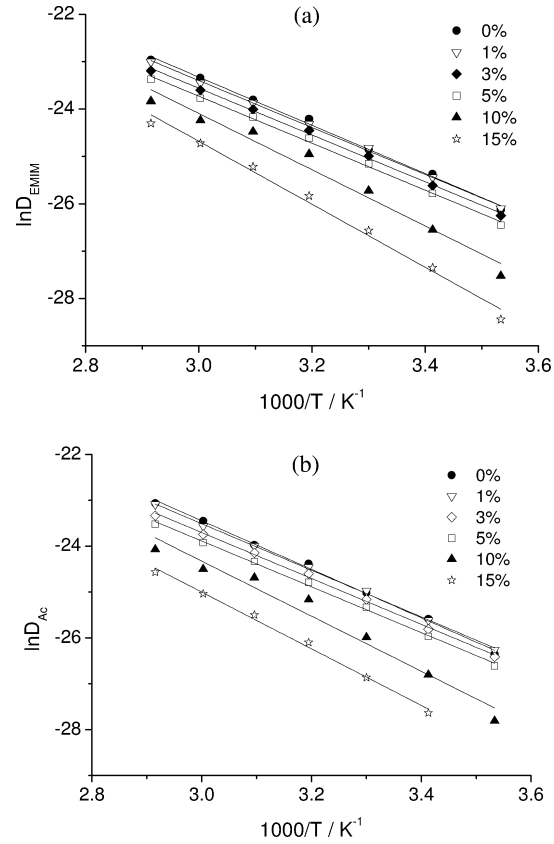

Figure 6. Logarithmic plots of the (a) $[EMIM]^+$ and (b) $[Ac]^-$ ion self-diffusion coefficients against reciprocal temperature for pure EMIMAc and each cellulose/EMIMAc solution. The lines are fits to eq 2. The error bars are approximately equal to the size of the data points used.

Table 1. Arrhenius Parameters Fit to the Temperature Dependences of the Ion Self-Diffusion Coefficients

cellulose weight percent (%)	$D_{iA}/10^{-4}$ m^2 s^{-1}		E_{iA}/kJ mol^{-1}	
	$[EMIM]^+$	$[Ac]^-$	$[EMIM]^+$	$[Ac]^-$
0	3 ± 1	5 ± 2	42 ± 1	43 ± 1
1	2.0 ± 0.5	2.6 ± 0.6	41 ± 1	42 ± 1
3	1.6 ± 0.5	1.7 ± 0.6	40 ± 1	42 ± 1
5	1.5 ± 0.5	1.4 ± 0.4	41 ± 1	42 ± 1
10	20 ± 2	20 ± 2	49 ± 4	50 ± 4
15	90 ± 8	20 ± 1	55 ± 2	51 ± 2

The activation energies for self-diffusion are typically larger in ILs than in both nonpolar and polar solvents, for example cyclohexane (13.7 kJ mol^{-1}) and DMSO (14.9 kJ mol^{-1}).[35] As seen from Table 1 the values of E_{iA} for the pure IL are 42 ± 1 and 43 ± 1 kJ mol^{-1} for the $[EMIM]^+$ and $[Ac]^-$ ions, respectively. The same value, around 40 kJ/mol, was found for EMIMAc from rheological measurements.[39] It is observed that the activation energies obtained from the Arrhenius analysis do not differ significantly between cation and anion within the range of cellulose concentrations studied.

3.4. Influence of Cellulose Concentration on Ion Diffusion. Figure 6 shows a significant reduction in the diffusivities of both the $[EMIM]^+$ and $[Ac]^-$ ions as the concentration of

cellulose is increased. This is what in general is observed for a solvent molecule diffusing in a polymer system. For a polymer solution one of the reasons for the diffusion coefficient to decrease with polymer concentration is the power-law increase of the solution viscosity.[39] It is important to describe the relationship between cellulose concentration and the ion diffusive behaviors to understand the transport properties and polymer−solvent interactions in these systems.

Theoretical treatments of solute diffusion in polymer−solvent systems are well-established in the literature. Several approaches such as obstruction, hydrodynamic and free-volume models are known; a detailed review is given by Masaro and Zhu.[45] Nothing though is known about solvent diffusion in cellulose-ionic liquid solutions. In our analysis we will visit one approach after another: Stokes−Einstein,[46] Maxwell−Fricke[47] and Mackie−Meares[48] obstruction models, free-volume theory due to Vrentas and Duda,[49] and Phillies' hydrodynamic model.[50]

In the following analyses the cellulose volume fraction was calculated using the expression

$$\phi = \frac{c_p/\rho_p}{c_E/\rho_E + c_p/\rho_p} \tag{3}$$

where c_p is the mass fraction of cellulose, c_E is the mass fraction of EMIMAc, $\rho_p = 1.5$ g cm^{-3} is the bulk density of cellulose, and $\rho_E = 1.1$ g cm^{-3} is the bulk density of EMIMAc, all taken at 25 °C.[34]

3.4.1. Stokes−Einstein Analysis. Correlations between the temperature dependences of the self-diffusion coefficients and viscosities of ILs have previously been analyzed[46] in terms of the Stokes−Einstein relationship

$$D_i(T) = \frac{kT}{6\pi\eta(T)R_{H,i}} \tag{4}$$

where $D_i(T)$ is the temperature dependent self-diffusion coefficient, k is the Boltzmann constant, $\eta(T)$ is the temperature dependent zero-shear viscosity of the IL solution, and $R_{H,i}$ is the effective hydrodynamic radius of the diffusing species. In Figure 7, panels a and b, we present logarithmic plots of $D_{EMIM}(T)$ and $D_{Ac}(T)$ against $T/\eta(T)$ for pure EMIMAc and each cellulose/EMIMAc solution in order to draw a comparison between data sets. The viscosity data for the same EMIMAc cellulose solutions as studied here have been taken from a recent publication by Sescousse et al.[39] The linear correlation in the experimental data with a slope approximately equal to unity (see insets) demonstrates that the Stokes−Einstein equation provides a suitable description of the relationship between $D_i(T)$ and $T/\eta(T)$ for pure EMIMAc. Deviations from the Stokes−Einstein relationship, i.e., departures from a slope equal to unity, are observed when the analysis is applied to the cellulose/EMIMAc solutions. The slopes for the data sets (see insets) tend to a value of ∼0.7 on increase of cellulose concentration.

Values obtained for the effective hydrodynamic radii, $R_{H,i}$, using the diffusion coefficients obtained and a conventional Stokes−Einstein analysis of pure EMIMAc were 1.6 Å and 1.8 Å for $[EMIM]^+$ and $[Ac]^-$ ions, respectively. These values are of the same order of magnitude as a value of 3 Å for the $[EMIM]^+$ derived from the ion molar volume reported by Seki et al.[51] and a value of 1.6 Å for the $[Ac]^-$ ion estimated using group contributions to the van der Waals molar volume.[52] The somewhat small cation radius derived from this analysis reflects

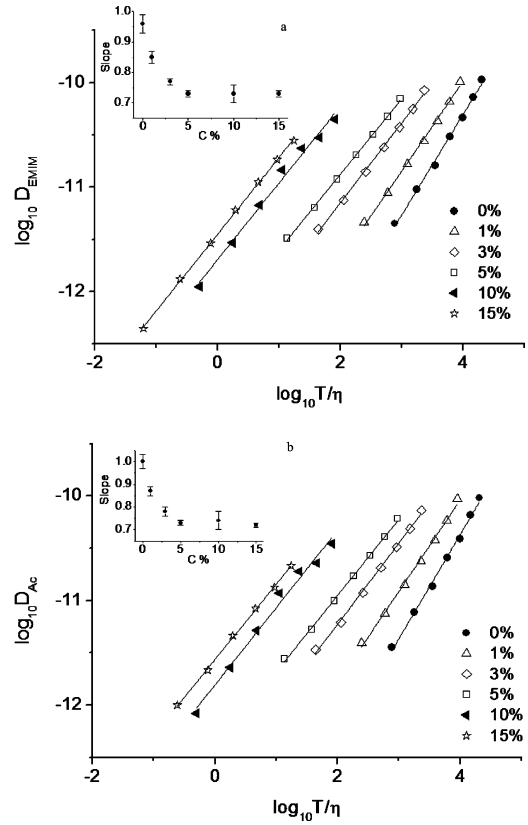

Figure 7. log−log plots of the (a) $[EMIM]^+$ ion and (b) $[Ac]^-$ ion self-diffusion coefficients against the ratio of temperature to viscosity for each cellulose/EMIMAc solution. The error bars are approximately equal to the size of the data points used. The graph inset in each plot shows the cellulose concentration dependence of the slope for each data set.

the known anomalous cation behavior; that is, it diffuses faster than its counterion.[53] Carper et al.[54] found from their Stokes−Einstein analysis that the $[EMIM]^+$ had a hydrodynamic radius between 1.16 and 2.00 Å depending on the particular system measured and the prefactor they used in eq 4. Interestingly this work and ours therefore suggests that it is not, as recently put forward,[55] the anion diffusing slowly but instead the cation diffusing faster than expected.

The Stokes−Einstein analysis and the deviation from the predicted eq 4 dependence caused by the addition of cellulose highlights that it is important to explore the role of cellulose on the diffusive behavior of the ions in more detail. The relationship between $[EMIM]^+$ and $[Ac]^-$ self-diffusion coefficients and cellulose concentration will now be explored.

3.4.2. Obstruction Models. Fricke[47] originally proposed the obstruction model (Maxwell−Fricke model) to analyze electrical conductivity in the presence of nonconducting regions. However the model has also been applied to the analysis of diffusion in polymer solutions and predicts the following relationship between the solvent diffusivity and polymer volume fraction

$$\frac{D}{D_0} = \frac{1-\phi'}{1+\phi'/\chi}\cdot\frac{1}{1-\phi} \tag{5}$$

where D is the self-diffusion coefficient of the solvent in solution, D_0 is the self-diffusion coefficient of the pure solvent, ϕ is the polymer volume fraction, ϕ' is the volume fraction of polymer plus nondiffusing solvent bound to the polymer, and

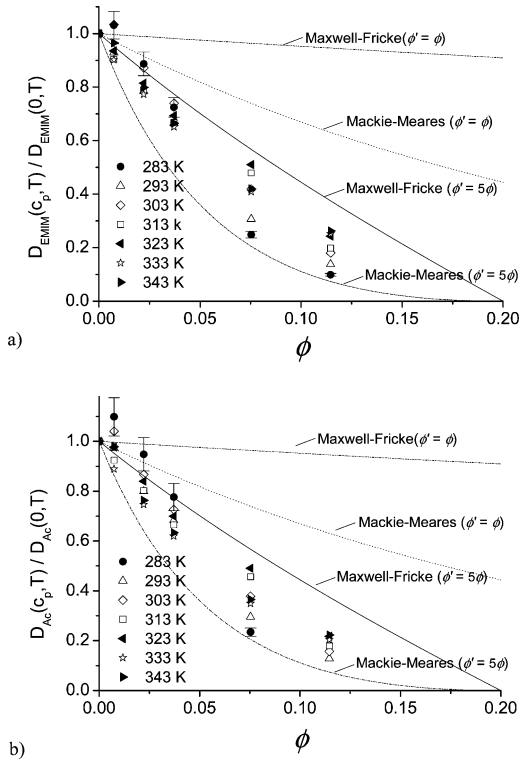

Figure 8. Experimental data and Maxwell−Fricke and Mackie−Meares obstruction models for the concentration dependence of the ratio of the self-diffusion coefficients in solution and the pure IL for (a) $[EMIM]^+$ and (b) $[Ac]^-$ ions. For clarity we have only displayed error bars for the 283 K data, the uncertainties in the other results are of a similar size.

χ is the shape parameter taking the value 2 for spherical obstructing regions.

Mackie and Meares[48] used the obstruction concept developed by Fricke to analyze the diffusion of electrolytes in a resin membrane. Their model based on a cubic array of lattice points, assuming equivalent sized polymer repeat and solute units, describes the concentration dependence of the diffusivity in terms of an increased tortuosity (or increased path-length), due to obstructions caused by "immobile" polymer chains. In particular the model has been successful in providing a simple account for the diffusivity of small solutes in polymer solutions and is given by

$$\frac{D}{D_0} = \left[\frac{1-\phi'}{1+\phi'}\right]^2 \tag{6}$$

where the terms are defined similarly for eq 5.

In Figure 8, panels a and b, a comparison is drawn between the concentration dependences of the ratios of the $[EMIM]^+$ and $[Ac]^-$ self-diffusion coefficients to their pure EMIMAc results and the predictions given by both Maxwell−Fricke and Mackie−Meares obstruction models. In the first instance we have applied the models assuming the absence of bound solvent, which implies $\phi = \phi'$. The findings are very similar to those of Mustafa et al.[56] in their work on aqueous (hydroxypropyl)cellulose where the retardation of the probe diffusivity increased with the polymer volume fraction at a rate comparable to that observed in this study. Neither the Maxwell−Fricke nor the Mackie−Meares models capture the concentration dependence of the solvent diffusive behavior when one assumes the absence of bound solvent.

Hydrogen bond formation between both $[EMIM]^+$ and $[Ac]^-$ ions with cellulose hydroxyl groups may be considered to yield an effective bound layer of solvent. Zhang et al.[31] concluded that in the primary solvation shell, the coordination of $[EMIM]^+$ and $[Ac]^-$ ions with cellobiose hydroxyl groups occurs in the approximate ratio 1:1:1 = $[EMIM]^+$:$[Ac]^-$:hydroxyl. Let us assume that this ratio describes the primary solvation shell for dissolved cellulose and that the densities of the bulk IL and solvation shell are equal. From this the total volume fraction of bound ions and cellulose can be estimated using

$$\frac{n_E}{n_H} = \frac{n_E}{3n_C} = \frac{1}{3}\left(\frac{M_C}{M_E}\frac{c_E}{c_p}\right) \tag{7}$$

and

$$\phi' = \phi_{Shell} + \phi = \frac{\left(\frac{n_H}{n_E}\frac{c_E}{\rho_E}\right) + c_p/\rho_p}{c_E/\rho_E + c_p/\rho_p} \tag{8}$$

where n_E is the molar quantity of EMIMAc, n_H is the molar quantity of cellulose hydroxyls, n_C is the molar quantity of the cellulose repeat unit (herein taken as $C_6H_{10}O_5$), M_E is the molar mass of EMIMAc (170 g mol^{-1}), M_C is the molar mass of the cellulose repeat unit (162 g mol^{-1}), and ϕ_{Shell} is the volume fraction occupied by EMIMAc in the primary solvation shell. Combining eqs 7 and 8 this predicts a relationship between polymer volume fraction and volume fraction of polymer plus nondiffusing bound solvent of $\phi' \approx 5\phi$. The fits taking $\phi' = 5\phi$ for both models are shown in Figure 8, panels a and b. The Maxwell−Fricke model underestimates the trend in the experimental data while an overestimate is given by the Mackie-Meares model. Despite a significant improvement in terms of the correlation between experiment and theory obtained, neither model can be considered to provide a satisfactory description of the cellulose concentration dependences of $[EMIM]^+$ and $[Ac]^-$ self-diffusion coefficients. Further adjustments to the model parameters (i.e., χ, ϕ_{Shell}, and ϕ') could of course be made to provide qualitatively good fits, but this would be a somewhat arbitrary tailoring in the absence of further experimental evidence.

From $\phi' \approx 5\phi$ it may also be inferred that once the volume fraction of cellulose within solution reaches a value of $\phi \approx 0.2$ (or mass fraction, $c_p \approx 0.27\%$), all of the EMIMAc units are "bound" in the primary solvation shell; the further dissolution of cellulose will therefore be inhibited. This value for the maximum cellulose concentration solubility is close to values reported in the literature for cellulose/EMIMAc solutions of ~23% *w/w*.[3] The analysis above is therefore considered to provide a reasonable first approximation for the volume fraction of bound ions.

3.4.3. Free-Volume Model. Free-volume is an important and established concept for understanding the self-diffusion in random coil polymer−solvent systems. Although cellulose chains are considered to be semiflexible, Mustafa et al.[56] report modest success for a free-volume model in their work on diffusion in aqueous (hydroxypropyl)cellulose solutions. The free-volume theory developed by Vrentas and Duda[49] was considered in this study as the model addresses both temperature and concentration dependences. Waggoner et al.[57] have demonstrated that for a binary system the Vrentas and Duda model may be simplified at low polymer concentrations to the form

$$\frac{D(c_p,T)}{D(0,T)} \approx \exp\left[-\frac{c_p \xi \hat{V}_p^*}{c_s \hat{V}_{fs}(T)/\lambda}\right] \quad (9)$$

where c_s and c_p are respectively the solvent and polymer mass fractions, $\hat{V}_p^*$ is the polymer specific critical free-volume, ξ corresponds to the ratio of solvent to polymer molar free-volume, λ is a constant which accounts for the overlap of solvent and polymer free-volumes, and $\hat{V}_{fs}(T)$ is the temperature dependent free-volume of the solvent "jumping" unit. The temperature dependence of the solvent molar free-volume is given by

$$\hat{V}_{fs}(T)/\lambda = K_{1s}[T + K_{2s} - T_{gs}]/\lambda \quad (10)$$

where $\lambda\hat{V}_s^*/K_{1s}$ and $K_{2s} - T_{gs}$ are constants which equate respectively to the Vogel−Tamman−Fulcher parameters B and T_0 derived from the temperature dependence of the solvent viscosity. It is convenient to also apply the following substitution in eq 9:

$$\xi = \frac{M_s^j}{M_p^j}\frac{\hat{V}_s^*}{\hat{V}_p^*} \quad (11)$$

where M_s^j and M_p^j are the molar masses of the solvent and polymer "jumping" units, respectively, and $\hat{V}_s^*$ is the solvent specific critical free-volume.

Following Vrentas and Duda[49] we have assumed the polymer "jumping" unit to be equivalent to the polymer repeat unit. For simplicity we treat the solutions as binary systems and take the solvent "jumping" unit as one EMIMAc molecule simply because the temperature dependent viscosity of the IL cannot be separated into components for each ion. Similarly in this free volume analysis (eq 9) we will use the $D(c,T)/D(0,T)$ values for the $[EMIM]^+$ ions. The equivalent ratios obtained for the $[Ac]^-$ ions show extremely similar trends.

The temperature dependent viscosity of EMIMAc has been analyzed elsewhere,[39] and we have taken the VTF parameters from that work. Table 2 records values for each of the parameters used in applying the Vrentas−Duda model and the corresponding predictions are compared with the experimental data in Figure 9.

The temperature dependence of the viscosity[39] has previously been shown to be characterized by the VTF equation; thus, free-volume might be anticipated to determine both the temperature and concentration dependences of the ion self-diffusion coefficients. It is clear from Figure 9 using the parameters given in Table 2 that this approach does not accurately capture the concentration dependences of the self-diffusion coefficients.

A key criterion[58,59] for the validity of the free-volume model is that the polymer chains physically overlap, with the semidilute cellulose solutions studied herein fulfilling this requirement for $c_p > 1-2\%$.[39] Additional complexities associated with these systems in terms of the ionic nature of EMIMAc and the interactions between $[EMIM]^+$ and $[Ac]^-$ ions, and cellulose, introduce elements which are not addressed by this free-volume model. The significance of such interactions may be the presiding factor that accounts for the failure of the Vrentas−Duda free-volume model.

3.4.4. Hydrodynamic Model. Cukier[60] derived a model to describe solvent diffusion in semidilute polymer solutions by considering hydrodynamic screening effects due to the overlap of the polymer chains. The dependence of the solvent diffusion coefficient on strength of the screening interaction is given by

$$D = D_0 \exp[-\kappa_H R_H] \quad (12)$$

where κ_H quantifies hydrodynamic screening interactions and R_H is the hydrodynamic radius of the solvent. In the semidilute regime Cukier found that the extent of hydrodynamic screening scaled with the square root of the polymer concentration ($\kappa_H \propto c_p^{1/2}$). Numerous studies in the literature based on the hydrodynamic interpretation have established a strong correlation between screening and polymer concentration. The value of the scaling exponent is however found not to be unique. This is demonstrated clearly by Phillies.[50]

Phillies[50] evaluated the results from studies on polymer and protein solutions arriving at the following empirical scaling equation for polymer self-diffusion

$$D = D_0 \exp[-\alpha c_p^{\nu}] \quad (13)$$

where α is a constant at a given temperature, c_p is the polymer concentration, and ν is a constant. The interpretation of Phillies is that the self-diffusion of the polymer chains can be described by eq 13. In this light Cukier's model is a special case of the Phillies generic expression with $\nu = 1/2$.

The significance of the parameter α and ν have been discussed in the literature, although no clear consensus has been reached on their physical interpretation.[45] In general α is considered to be related to the hydrodynamic radius, R_H, of the diffusing species. The relationship $\alpha \propto R_H$ is given by Cukier's hydrodynamic model. Phillies postulates $\alpha \propto R_H/a_0$ where a_0 is the closest distance between the diffusant and polymer.

Earlier mentioned rheological studies of cellulose/EMIMAc solutions have demonstrated that the critical cellulose overlap

Table 2. Vrentas−Duda Free-Volume Parameters Evaluated for EMIMAc from the Temperature Dependence of Zero-Shear Viscosity Reported by Sescousse et al.[39]

parameters	values
$K_{1s}/\lambda\hat{V}_s^*/K^{-1}$	2.86×10^{-3}
$K_{2s} - T_{gs}/K$	−216
$M_s^j/g\ mol^{-1}$	170
$M_p^j/g\ mol^{-1}$	162

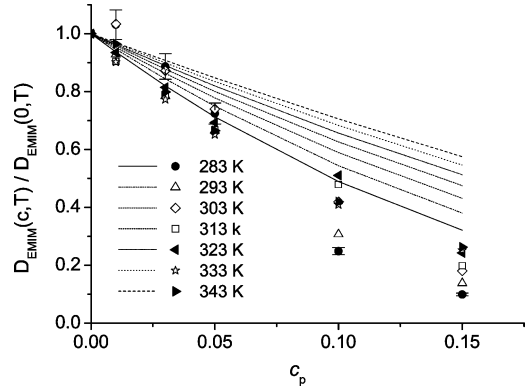

Figure 9. Concentration dependence of the ratio of $[EMIM]^+$ self-diffusion coefficients in solution to the pure IL with the predictions of the Vrentas−Duda free volume model using the parameters given in Table 2. For clarity we have only displayed error bars for the 283 K data, the uncertainties in the other results are of a similar size.

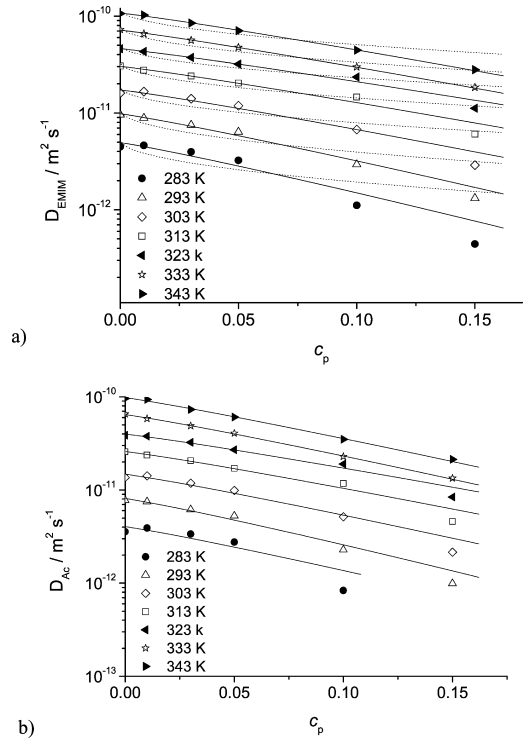

Figure 10. Phillies hydrodynamic model for concentration dependences of the a) $[EMIM]^+$ ion and b) $[Ac]^-$ ion self-diffusion coefficients in each solution. Dotted lines correspond to $\nu = 1/2$ (see eq 13) and solid lines to $\nu = 1.1$. The error bars are approximately equal to the size of the data points used.

Table 3. Values for the Parameter α Evaluated Using Phillies Hydrodynamic Model with the Exponent $\nu = 1.1$

	α		
temperature/K	$[EMIM]^+$	$[Ac]^-$	$\alpha_{EMIM}/\alpha_{Ac}$
283	15 ± 3	14 ± 4	1.1 ± 0.4
293	14 ± 1	14 ± 2	1.0 ± 0.2
303	12 ± 1	13 ± 2	0.9 ± 0.2
313	11 ± 1	11 ± 2	1.0 ± 0.2
323	9.9 ± 0.8	10.6 ± 0.9	0.9 ± 0.1
333	11.1 ± 0.3	12.9 ± 0.4	0.86 ± 0.04
343	11.1 ± 0.3	12.7 ± 0.6	0.87 ± 0.05

concentration, c_p^*, is ~1% *w/w* at 20 °C.[39] Hydrodynamic interactions may therefore significantly influence ion diffusion in the range of cellulose concentrations studied. We used $\nu = 1.1$ after inspecting Phillies evaluation for the molecular weight dependence of the exponent for numerous polymer and protein solutions, for which the generic relationship $\nu \propto (\bar{M}_w)^{-1/4}$ was established (here the microcrystalline cellulose is of DP = 180).

In Figure 10 the data have been fit using the hydrodynamic model given by eq 13. Although the range of concentrations is limited, each data set is reasonably described by the stretched-exponential decay. In particular using $\nu = 1.1$ captures the subtle curvature in the concentration dependence of the self-diffusion coefficients that is seen on the semilogarithmic scale. The case where $\nu = 1/2$ (in eq 13) has also been fit to the data in Figure 10a (shown by dotted lines); however, the quality of each fit is poor by comparison. Values for the fitting parameter α are listed in Table 3 for the case when $\nu = 1.1$.

It is noted that the average values for α are slightly smaller for the $[EMIM]^+$ ion compared to the $[Ac]^-$ ion. This observation is seen to be consistent with the interpretation of α in terms of the hydrodynamic radii of the ions by comparing the ratio, $R_{H,EMIM}/R_{H,Ac} \approx 0.9$ (from Stokes−Einstein analysis), with values for the ratio, $\alpha_{EMIM}/\alpha_{Ac}$ given in Table 3.

Phillies hydrodynamic model does capture the concentration dependence of the self-diffusion coefficients and this has been demonstrated through the evaluation of ν using the cellulose molecular weight.

4. Conclusions

Solutions of cellulose (0−15% *w/w*) in 1-ethyl-3-methylimidazolium acetate (EMIMAc) have been investigated using pulsed-field gradient NMR. EMIMAc flows at ambient temperature, has very low vapor pressure and high thermal stability, and thus it is potentially a very attractive solvent for cellulose processing. This NMR study coupled with recently published rheological results on the same system enabled a better understanding of the solution structure−property relationships that are needed for practical applications. For these samples the ^1H spectra and self-diffusion coefficients of both the cation and anion have been determined in the range 10 to 70 °C. The dependences of the ^1H NMR spectral band chemical shifts on cellulose concentration were found to be consistent with a recent NMR study on cellobiose/EMIMAc solutions,[31] which was used as a model system to understand cellulose dissolution in EMIMAc.

We did not observe multiple spectral bands for each ^1H species that would indicate associated and dissociated ion states. Therefore any exchange between isolated ions, ion pairs and ion aggregates (if they exist) must occur on a time-scale shorter than that set by the NMR experiment (i.e., 10^{-8}−10^{-9} s).

The linear dependence of the logarithm of signal intensity on the square of the gradient strength revealed that on the time-scale of the diffusion measurements (10−60 ms), the ions can be considered to experience a homogeneous environment. There was no evidence for phase separation as we did not observe biexponential decays that would indicate structurally distinct regions each with their own characteristic diffusivity.

The physically smaller $[Ac]^-$ anion was found to have a slower diffusivity than the larger $[EMIM]^+$ cation. Intriguingly the difference in the cation and anion self-diffusion coefficients further increased on the addition of cellulose.

The self-diffusion coefficients and zero-shear viscosity[39] of pure EMIMAc were found to be consistent with the Stokes−Einstein relationship, giving the hydrodynamic radii 1.6 and 1.8 Å for $[EMIM]^+$ and $[Ac]^-$, respectively. As would be expected systematic deviations from this relationship were observed when the same analysis was applied to the EMIMAc/cellulose solutions, due to the ions interacting with the cellulose.

The temperature dependences of the self-diffusion coefficients were well described by an Arrhenius behavior in the temperatures interval studied. This gave activation energies as a function of cellulose concentration (40−55 kJ/mol). For the pure solvent the activation energies determined from the diffusion measurements and from the viscosity data[39] were found to be equal.

We applied a variety of models (obstruction, free-volume, and hydrodynamic) to describe the effect of polymer concentration on the diffusion of the solvent molecules. The presence of bound solvent was deduced from the obstruction models of Maxwell−Fricke and Mackie−Meares. This proportion of bound ions found was used to predict the maximum possible concentration of cellulose dissolution (~27% *w/w*), which agreed remarkably well with other studies.[3] The Vrentas−Duda free-volume model was found to not yield a satisfactory

agreement between experiment and theory. The Phillies hydrodynamic model, approached by applying an empirical relationship for the exponent, $\nu \propto \bar{M}_w^{-1/4}$, provided a good quantitative agreement with the concentration dependences of the ion self-diffusion coefficients.

Acknowledgment. Part of this work was made possible by a Royal Society International Outgoing Short Visit Grant 2008/R3. We would like to thank Simon Wellings (School of Physics and Astronomy, University of Leeds, U.K.) for his help in sample preparation.

References and Notes

(1) Ober, C. K.; Cheng, S. Z. D.; Hammond, P. T.; Muthukumar, M.; Reichmanis, E.; Wooley, K. L.; Lodge, T. P. *Macromolecules* **2009**, *42*, 465–4721.
(2) Zhou, J.; Chang, C.; Zhang, R.; Zhang, L. *Macromol. Biosci.* **2007**, *7*, 804–809.
(3) Pinkert, A.; Marsh, K. N.; Pang, S.; Staiger, M. P. *Chem. Rev.* **2009**, *109*, 6712–6728.
(4) Fink, H. P.; Weigel, P.; Purz, H. J.; Ganster, J. *Prog. Polym. Sci.* **2001**, *26*, 1473–1524.
(5) Dawsey, T. R.; McCormick, C. L. *J. Macromol. Sci.-Rev. Macromol. Chem. Phys.* **1990**, *C30*, 405–440.
(6) Kohler, S.; Heinze, T. *Macromol. Biosci.* **2007**, *7*, 307–314.
(7) Fischer, S.; Leipner, H.; Thummler, K.; Brendler, E.; Peters, J. *Cellulose* **2003**, *10*, 227–236.
(8) Thummler, K.; Fischer, S.; Peters, J.; Liebert, T.; Heinze, T. *Cellulose* **2010**, *17*, 161–165.
(9) Roy, C.; Budtova, T.; Navard, P. *Biomacromolecules* **2003**, *4*, 259–264.
(10) Cai, J.; Zhang, L. *Biomacromolecules* **2006**, *7*, 183–189.
(11) Cuculo, J. A.; Smith, C. B.; Sangwatanaroj, U.; Stejskal, E. O.; Sankar, S. S. *J. Polym. Sci. Part A-Polym. Chem.* **1994**, *32*, 229–239.
(12) Frey, M. W.; Li, L.; Xiao, M.; Gould, T. *Cellulose* **2006**, *13*, 147–155.
(13) Rosenau, T.; Potthast, A.; Sixta, H.; Kosma, P. *Prog. Polym. Sci.* **2001**, *26*, 1763–1837.
(14) Welton, T. *Chem. Rev.* **1999**, *99*, 2071–2083.
(15) Armand, M.; Endres, F.; MacFarlane, D. R.; Ohno, H.; Scrosati, B. *Nat. Mater.* **2009**, *8*, 621–629.
(16) Han, X.; Armstrong, D. W. *Acc. Chem. Res.* **2007**, *40*, 1079–1086.
(17) Zhu, S. D.; Wu, Y. X.; Chen, Q. M.; Yu, Z. N.; Wang, C. W.; Jin, S. W.; Ding, Y. G.; Wu, G. *Green Chem.* **2006**, *8*, 325–327.
(18) Holbrey, J. D.; Seddon, K. R. *J. Chem. Soc.-Dalton Trans.* **1999**, 2133–2139.
(19) Okoturo, O. O.; VanderNoot, T. J. *J. Electroanal. Chem.* **2004**, *568*, 167–181.
(20) El Seoud, O. A.; Koschella, A.; Fidale, L. C.; Dorn, S.; Heinze, T. *Biomacromolecules* **2007**, *8*, 2629–2647.
(21) Cai, T.; Zhang, H. H.; Guo, Q. H.; Shao, H. L.; Hu, X. C. *J. Appl. Polym. Sci.* **2010**, *115*, 1047–1053.
(22) Kuang, Q. L.; Zhao, J. C.; Niu, Y. H.; Zhang, J.; Wang, Z. G. *J. Phys. Chem. B* **2008**, *112*, 10234–10240.
(23) Wendler, F.; Kosan, B.; Krieg, M.; Meister, F. *Macromol. Symp.* **2009**, *280*, 112–122.
(24) Zhang, H.; Wu, J.; Zhang, J.; He, J. S. *Macromolecules* **2005**, *38*, 8272–8277.
(25) Zhao, Q.; Yam, R.; Zhang, B. Q.; Yang, Y. K.; Cheng, X. J.; Li, R. *Cellulose* **2009**, *16*, 217–226.
(26) Zhao, Y.; Gao, S.; Wang, J.; Tang, J. *J. Phys. Chem. B* **2008**, *112*, 2031–2039.
(27) Tokuda, H.; Tsuzuki, S.; Susan, M.; Hayamizu, K.; Watanabe, M. *J. Phys. Chem. B* **2006**, *110*, 19593–19600.
(28) Noda, A.; Hayamizu, K.; Watanabe, M. *J. Phys. Chem. B* **2001**, *105*, 4603–4610.
(29) Freire, M. G.; Carvalho, P. J.; Silva, A. M. S.; Santos, L.; Rebelo, L. P. N.; Marrucho, I. M.; Coutinho, J. A. P. *J. Phys. Chem. B* **2009**, *113*, 202–211.
(30) Remsing, R. C.; Swatloski, R. P.; Rogers, R. D.; Moyna, G. *Chem. Commun.* **2006**, 1271–1273.
(31) Zhang, J. M.; Zhang, H.; Wu, J.; Zhang, J.; He, J. S.; Xiang, J. F. *Phys. Chem. Chem. Phys.* **2010**, *12*, 1941–1947.
(32) Stejskal, E. O.; Tanner, J. E. *J. Chem. Phys.* **1965**, *42*, 288–292.
(33) Morris, K. F.; Johnson, C. S. *J. Am. Chem. Soc.* **1992**, *114*, 3139–3141.
(34) Gericke, M.; Schlufter, K.; Liebert, T.; Heinze, T.; Budtova, T. *Biomacromolecules* **2009**, *10*, 1188–1194.
(35) Holz, M.; Heil, S. R.; Sacco, A. *Phys. Chem. Chem. Phys.* **2000**, *2*, 4740–4742.
(36) Annat, G.; MacFarlane, D. R.; Forsyth, M. *J. Phys. Chem. B* **2007**, *111*, 9018–9024.
(37) Cotts, R. M.; Hoch, M. J. R.; Sun, T.; Markett, J. T. *J. Magn. Reson.* **1989**, *83*, 252–266.
(38) Dhumal, N. R.; Kim, H. J.; Kiefer, J. *J. Phys. Chem. A* **2009**, *113*, 10397–10404.
(39) Sescousse, R.; Le, K. A.; Ries, M. E.; Budtova, T. *J. Phys. Chem. B* **2010**, *114*, 7222–7228.
(40) Tokuda, H.; Hayamizu, K.; Ishii, K.; Abu Bin Hasan Susan, M.; Watanabe, M. *J. Phys. Chem. B* **2004**, *108*, 16593–16600.
(41) Tokuda, H.; Hayamizu, K.; Ishii, K.; Susan, M.; Watanabe, M. *J. Phys. Chem. B* **2005**, *109*, 6103–6110.
(42) Tokuda, H.; Ishii, K.; Susan, M.; Tsuzuki, S.; Hayamizu, K.; Watanabe, M. *J. Phys. Chem. B* **2006**, *110*, 2833–2839.
(43) Tsuzuki, S.; Shinoda, W.; Saito, H.; Mikami, M.; Tokuda, H.; Watanabe, M. *J. Phys. Chem. B* **2009**, *113*, 10641–10649.
(44) Urahata, S. M.; Ribeiro, M. C. C. *J. Chem. Phys.* **2005**, *122*, 9.
(45) Masaro, L.; Zhu, X. X. *Prog. Polym. Sci.* **1999**, *24*, 731–775.
(46) Umecky, T.; Kanakubo, M.; Ikushima, Y. *Fluid Phase Equilib.* **2005**, *228*, 329–333.
(47) Fricke, H. *Phys. Rev.* **1924**, *24*, 575–587.
(48) Mackie, J. S.; Meares, P. *Proc. R. Soc. London Ser. A-Math. Phys. Sci.* **1955**, *232*, 498–509.
(49) Vrentas, J. S.; Duda, J. L. *J. Polym. Sci., Part B: Polym. Phys.* **1977**, *15*, 403–416.
(50) Phillies, G. D. J. *Macromolecules* **1986**, *19*, 2367–2376.
(51) Seki, S.; Kobayashi, T.; Kobayashi, Y.; Takei, K.; Miyashiro, H.; Kikuko, H.; Tsuzuki, S.; Mitsugi, T.; Umebayashi, Y. *J. Mol. Liq.* **2010**, *152*, 9–13.
(52) van Krevelen, D. W.; te Nijenhuis, K. *Properties of polymers: their correlation with chemical structure; their numerical estimation and prediction from additive group contributions*, 4th ed.; Elsevier: Amsterdam, 2009.
(53) Menjoge, A.; Dixon, J.; Brennecke, J. F.; Maginn, E. J.; Vasenkov, S. *J. Phys. Chem. B* **2009**, *113*, 6353–6359.
(54) Carper, W. R.; Mains, G. J.; Piersma, B. J.; Mansfield, S. L.; Larive, C. K. *J. Phys. Chem.* **1996**, *100*, 4724–4728.
(55) Remsing, R. C.; Hernandez, G.; Swatloski, R. P.; Massefski, W. W.; Rogers, R. D.; Moyna, G. *J. Phys. Chem. B* **2008**, *112*, 11071–11078.
(56) Mustafa, M. B.; Tipton, D. L.; Barkley, M. D.; Russo, P. S.; Blum, F. D. *Macromolecules* **1993**, *26*, 370–378.
(57) Waggoner, R. A.; Blum, F. D.; Macelroy, J. M. D. *Macromolecules* **1993**, *26*, 6841–6848.
(58) Vrentas, J. S.; Duda, J. L. *J. Polym. Sci., Part B: Polym. Phys.* **1977**, *15*, 417–439.
(59) Vrentas, J. S.; Duda, J. L.; Ling, H. C.; Hou, A. C. *J. Polym. Sci., Part B: Polym. Phys.* **1985**, *23*, 289–304.
(60) Cukier, R. I. *Macromolecules* **1984**, *17*, 252–255.

BM1006807